

# Mixing Temperature Measurement of Swirl Cold Flow Exiting Cold Exit of Vortex Tube

Mohd Hazwan bin Yusof<sup>1,a</sup> and Hiroshi Katanoda<sup>2</sup>

<sup>1</sup>Faculty of Mechanical Engineering, Universiti Malaysia Pahang, 26600, Pekan, Pahang, Malaysia

<sup>2</sup>Graduate School of Science and Engineering, Kagoshima University, 1-21-40 Korimoto, Kagoshima 890-0065, Japan

**Abstract.** Cold flow of a vortex tube exiting the tube with a swirl flow movement produces a temperature distribution at the cold exit. In order to measure the mixing temperature of a swirl cold flow exiting cold exit of vortex tube, a simple mixing chamber is created using pipe and copper mesh. It is observed through this experiment that the temperature differences between inlet and cold flow increases when the cold fraction is decreased from 1.0. In addition, the temperature differences between inlet and cold flow increases when the inlet pressure is increased from 0.2 MPa to 0.5 MPa. The maximum value of cooling capacity in this research is obtained at inlet pressure of 0.5MPa and cold fraction of 0.4.

## 1 Introduction

A Vortex Tube (VT) is a simple and useful fluid dynamic device, used to obtain both cold and hot flows from a compressed gas at room temperature. It can produce a cold flow measuring around -30°C, and a hot flow of up to around 130°C. In 1930's, Ranque was the first to have discovered the energy/temperature separation phenomenon [1]. Later in 1947, the flow mechanism of the vortex tube was investigated by Hilsch [2]. Since then, the vortex tube is also known as The Ranque-Hilsch Vortex Tube (RHVT).

There are a lot of advantages to VT, such as being light, small, with no moving parts, maintenance free, and an instant supply of cold flow. But, VT has low thermal efficiency and low coefficient of performance (COP).

The VT has been mainly used as a device to cool small area, for example, electrical devices, thermal sensors, controlling cabins, cutting tools and areas under thermal stresses [3]. In addition to that, VT is also expected to be used as an oxygen collector of aero-propulsion engine for a subsonic-to-supersonic vehicle in in-flight condition [4], or as a device to clean exhaust gas of an internal combustion engine [5].

There are two types of VT as shown in Fig. 1. Figure 1(a) shows a Uni-flow VT which consists of a vortex chamber, multiple or a single inlet nozzle, a control valve, and a tube. The center of the control valve at the end of the tube is an exit where a cold flow is discharged (cold exit). The peripheral area of the control valve is another exit where a hot flow is discharged (hot exit). Figure 1(b) shows a Counter-flow VT which consists of a vortex chamber, multiple or a single inlet nozzle, a control valve, and a tube. The cold exit is located at the

center of the tube near inlet nozzle and hot exit is located at the peripheral of control valve at the other end. According to previous researches [6-7], the performance of the counter-flow VT is better than the uni-flow VT. Therefore, in this research, we focus on the counter-flow VT.

Next, a generally thought to occur flow pattern inside the counter-flow VT is explained. It should be noted that several flow patterns is proposed by several researchers. As was shown in Fig. 1(b), compressed air enters a VT through a single or multiple tangential nozzles, and a high-speed vortical flow is generated in the vortex chamber. A part of the rotational flow follows the tube wall towards the opposite end; hot end. Then, this flow exits as a hot flow at the hot exit. The core flow is forced back towards the vortex chamber by a control valve, and exits as a cold flow at the cold exit. The temperatures of cold and hot flows can be changed by adjusting a cold fraction  $\varepsilon$ , which is a ratio of the mass flow rate of a cold flow,  $\dot{m}_{cold}$ , to the inlet mass flow rate,  $\dot{m}_{in}$ ;

$$\varepsilon = \frac{\dot{m}_{cold}}{\dot{m}_{in}} \quad (1)$$

The cold fraction is adjusted by axially moving the control valve left or right. From the definition of Eq. (1), the cold fraction value varies from 0 to 1. Cold fraction  $\varepsilon = 0$  means, no flow exits from the cold exit, and  $\varepsilon = 1$  means all flow inside the tube is discharged from the cold exit.

Several numerical and experimental works had been done to investigate the performance of the VT. Saidi et al.[8] studied the effects of parameter on the performance of VT by changing diameter and length of main tube, diameter of cold exit, shape of entrance nozzle, and types of working gas. They used a tube with an inner diameter of 18 mm. They reported the optimum values of length to

<sup>a</sup> Corresponding author: mohdhazwan@ump.edu.my

inner diameter ratio ( $L/D$ ) is 55.5, cold exit diameter is 50% of inner diameter of tube, and diameter of inlet nozzle is 3.5 mm with 3 inlets. They also reported that helium is better than oxygen or air as the working gas for a higher performance of VT. Behera et al.[9] performed a Computational Fluid Dynamics (CFD) analysis and experimental investigation to optimize the geometry of VT. They reported that the optimum size of the cold exit is 58% of the diameter of the tube. Nimbalkar et. al. [10] performed similar experiments to determine the optimum size of the cold exit. They reported that the optimum diameter of the cold exit is 50% of the diameter of the tube, which is same as Saidi et al.[8] but 8% smaller than the result of Behera et al.[9]. Wu et al.[11] proposed a new nozzle with an equal Mach number gradient and flow velocity at the inlet nozzle. They reported that the cooling effect with the new nozzle is improved compared to the conventional nozzle. Aydin et al.[12] proposed a new helical type of vortex generator for a counter-flow VT. They reported that the new helical type of vortex generator has an obvious and superior effect on temperature separation with a temperature difference between cold flow and inlet flow is up to be 45.5°C at inlet pressure of 0.5MPa. Markal et al.[13] investigated the effect of the control valve's head angle of a counter-flow VT. They reported that this effect is generally negligible in a large length to tube inner diameter ratio. Chang et al.[14] investigated the effect of a divergent vortex chamber to the performance of the VT, with variation of divergent angle of tube. They reported that the performance of the VT can be improved by using the divergent tube with a divergent angle not more than 6°. Avci[15] studied the effects, of nozzle aspect ratio and the nozzle number of a helical vortex generator, on the performance of the VT. He reported that the temperature difference increases with increasing nozzle aspect ratio and single nozzle leads to better performance than the VT with 2 and 3 nozzles.

Until now, most researchers measured the cold flow temperature by inserting a thermocouple into a pipe which connects the cold exit with mass flow meter. It is well known that the cold flow exits cold exit in swirl flow movement. In addition, a reversed flow is observed at the cold exit, experimentally [16]. Thus, a radial temperature distribution exists at the cold exit. To validate the performance of VT, a proper measurement of cold flow temperature is needed. In this research, a mixing chamber is created and installed at the end of cold exit to extinguish the radial temperature distribution at cold exit. The measured mixing temperature is used to determine the cooling capacity of VT.

## 2 Experimental Procedure

Figure 2 shows a schematic diagram of the experimental setup of our VT. Compressed air up to 1MPa is supplied to the vortex chamber of the VT (10), through mass flow meters (1), stagnation chamber (3) and pressure control valve (4). Then, a vortical flow is generated through the inlet tangential nozzles. The cold flow exit is located near the inlet of the tangential nozzles, the left end of the VT

in the figure. The hot flow exit is at the opposite end of the tube. The inlet temperature and pressure were measured by temperature/humidity sensor (11) and digital manometer (5), respectively. The inlet pressures were kept constant in the range of 0.2~0.5MPa. The flow temperature discharged from the cold exit were measured by total temperature probe (12).

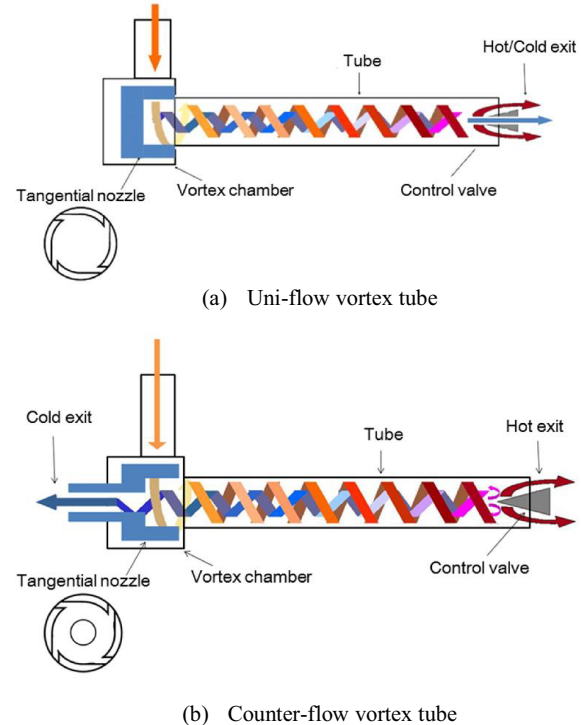


Figure 1. Classification of vortex tube.

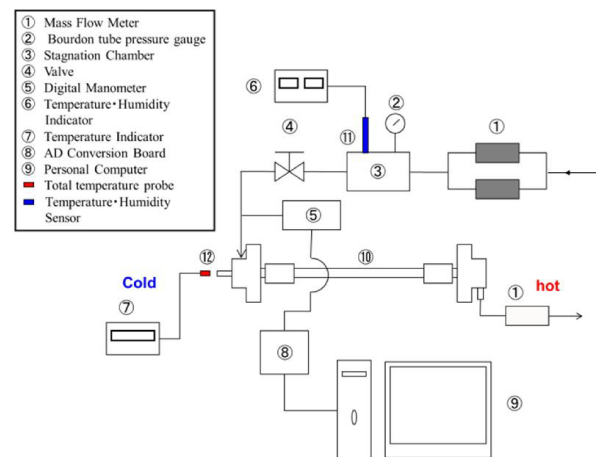
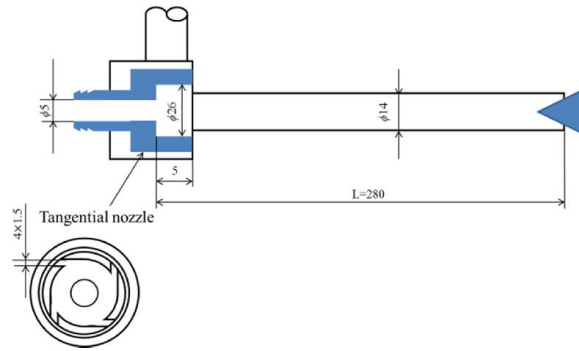
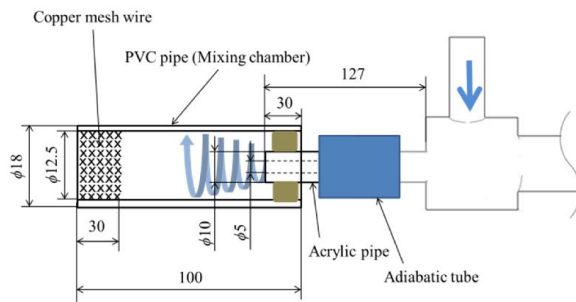


Figure 2. Experimental setup.

The dimensional details of the VT used in this research are shown in Fig. 3. It has an inner tube diameter  $D=14\text{mm}$  and a length to inner diameter ratio  $L/D=20$ , a cold exit diameter  $d_c=5\text{mm}$ , and four tangential nozzles.



**Figure 3.** Structure of vortex tube.



**Figure 4.** Schematic diagram of the experimental setup for measuring mixing temperature of cold flow.

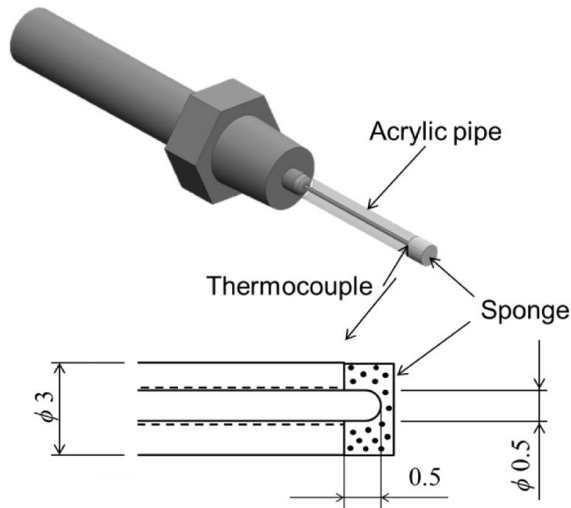


**Figure 5.** Total-temperature probe.

To evaluate the performance of VT, mixing temperature of cold and hot flows were measured. Due to the existence of radial temperature distribution at cold exit, a mixing chamber is installed at the cold exit as shown in Fig. 4 to measure the mixing temperature. As is indicated in this figure, an acrylic pipe, which was

inserted into a PVC pipe, was attached to the cold exit through an adiabatic tube. It should be noted that the inner diameter of acrylic pipe is equal to the diameter of cold exit ( $d_c = 5\text{ mm}$ ). A copper mesh wire was installed at the exit end of the PVC pipe. This copper mesh was used to enhance mixing of the cold flow, which was discharged from the acrylic pipe.

In this research, a specially created Total Temperature Probe is used to decelerate the flow and to measure the total temperature of the cold flow, as shown in Fig. 4. It is made by inserting a T-type  $\phi 0.5$  thermocouple, into an acrylic pipe, which has inner/outer diameter of 0.6/3.0 mm and length of 21.5 mm. Approximately 0.5 mm of the tip of the thermocouple is protruding from the rod, and 1 mm of the tip is covered with a sponge, to create a stagnation state during the measurement period. We investigated, the total temperature measurement error of the probe, by inserting the probe into a center line of a potential core region of a room temperature air jet, discharged from a converging nozzle with an exit diameter of 10 mm. The stagnation pressure was varied in the range of 0.12 to 0.20 MPa. The result shows that the measurement error of the total temperature probe is within  $\pm 1.0\text{ K}$ .

To assure the uniformity of radial temperature distribution at the cold exit after installing the mixing chamber, total temperature was measured at 5 different radial points at the end of the mixing chamber, as shown in Fig. 6.

The experimental conditions are summarized in Table 1.

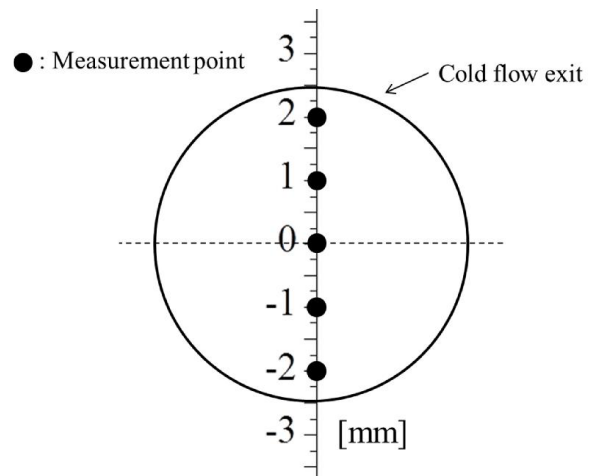


**Figure 6.** Measurement points of temperature distribution.

**Table 1.** Experimental conditions.

Inlet pressure, [MPa]	0.2~0.5 (0.1 increment)
Cold fraction, $\varepsilon$	0.1~0.9 (0.1 increment)
Working gas	Air

The performance of the VT is generally determined by the total-temperature difference between the inlet temperature,  $T_{in}$ , and the cold flow total temperature,  $\bar{T}_{t,cold}$ , that is;

$$\Delta\bar{T}_{t,cold} = T_{in} - \bar{T}_{t,cold} \quad (2)$$

The cooling performance of the VT is defined by the following equation;

$$\dot{Q}_c = \dot{m}_{cold} c_p \Delta\bar{T}_{t,cold} \quad (3)$$

where  $\dot{m}_{cold}$  is the mass flow rate of cold flow,  $c_p$  is the specific heat at constant pressure.

In this study, Eqs. (2) and (3) are used to evaluate the cold flow performance of the VT.

### 3 Results and Discussions

To assure that the cold flow is properly mixed, measurement were taken at 5 different radial points at the end of the mixing chamber during the experiments. The result is shown in Fig. 7. The horizontal axis of the figure shows the radial position from the center,  $x$ , and the vertical axis shows the measured temperature,  $\bar{T}_e$ . The result shows that negligible temperature fluctuation, within  $0.4^\circ\text{C}$ , exists at the end of the PVC pipe. From the result, it is understood that the cold flow is well mixed and the mixing total temperature of the cold flow can be obtained using the mixing chamber.

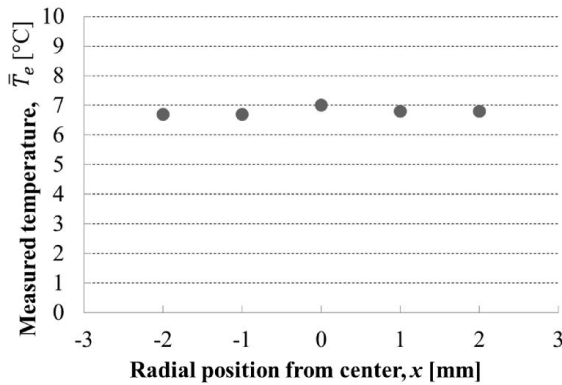


Figure 7. Radial temperature distribution at the end of mixing chamber.

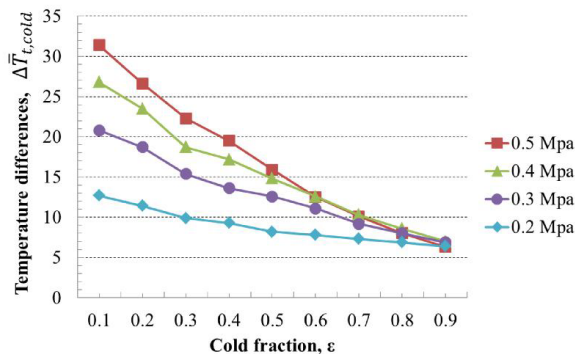


Figure 8. Mixing temperature of cold flow.

The mixing temperature of cold flow for  $p_{in} = 0.2 \sim 0.5\text{MPa}$ ,  $\epsilon = 0.1 \sim 0.9$  are shown in Fig. 8. The horizontal axis of the figure shows the cold fraction,  $\epsilon$ , and the vertical axis shows the temperature difference of mixing cold flow,  $\Delta\bar{T}_{t,cold}$ . It can be seen from this figure that  $\Delta\bar{T}_{t,cold}$  increases as the cold fraction decreases. This is due to the mixing of a hotter flow with a smaller mass flow rate at the peripheral region, with a colder flow with a larger mass flow rate at the central core of the tube, as the cold fraction decreases. When the inlet pressure is increased from 0.2 to 0.5 MPa,  $\Delta\bar{T}_{t,cold}$  increases at an arbitrary cold fraction. The tangential velocity of the vortex inside the tube increases when the inlet pressure increases, which enhance the energy/temperature separation phenomenon, causing a lower temperature of flow at the center of the tube. It can be concluded that, to obtain a lower temperature of cold flow, the value of cold fraction should be smaller and inlet pressure should be larger.

Figure 9 shows the cooling capacity of the VT. The horizontal axis of the figure shows the cold fraction,  $\epsilon$ , and the vertical axis shows the cooling capacity,  $\dot{Q}_c$  [W]. From this figure, it can be understood that cooling capacity increases as the inlet pressure increases. At  $p_{in} = 0.3 \sim 0.5\text{MPa}$ , when the cold fraction decreases from 1, the cooling capacity increases until it reaches a maximum value, then cooling capacity decreases to 0 at  $\epsilon = 0$ . Cooling capacity decreases at a small cold fraction due to the decrease in the mass flow rate of cold flow. The maximum value of cooling capacity in this research is obtained at  $p_{in} = 0.5\text{MPa}$  and  $\epsilon = 0.4$ .

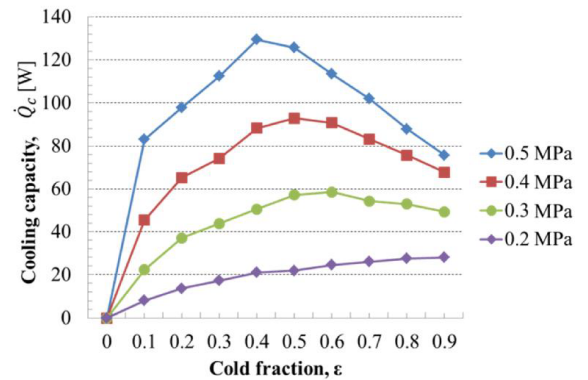


Figure 9. Cooling capacity of vortex tube.

### 4 Conclusions

An experimental study of the counter-flow vortex tube is conducted, in order to clarify the mixing temperature of swirl cold flow and the performance of vortex tube. The results obtained in this study are summarized as follows;

- 1) The radial temperature fluctuation at the end of mixing chamber is negligibly small, which is within  $0.4^\circ\text{C}$ .
- 2)  $\Delta\bar{T}_{t,cold}$  increases as the cold fraction decreases.

- 3) When the inlet pressure is increased from 0.2 to 0.5 MPa,  $\Delta \bar{T}_{t,cold}$  increases at an arbitrary cold fraction.
- 4) When the cold fraction is decreased from 1, the cooling capacity increases until it reaches a maximum value, then cooling capacity decreases to 0 at  $\varepsilon = 0$ .
- 5) The maximum value of cooling capacity in this research is obtained at  $p_{in} = 0.5\text{MPa}$  and  $\varepsilon = 0.4$ .

## References

1. G.J. Ranque, Experiences Sur la Detente Giratoire Avec Productions Simultanees d'un Echappement d'Air Chaud et d'un Echappement d'Air Froid, *Journal de Physique et Le Radium*, Vol.4, 1933, pp.112–114.
2. R. Hilsch, The Use of Expansion of Gases in a Centrifugal Field as Cooling Process, *The Review of Scientific Instruments*, Vol.18, pp.108–113, (1947).
3. S. Eiamsa-ard and P. Promvonge, Review of Ranque-Hilsch Effects in Vortex Tubes, *Renewable and Sustainable Energy Rev.*, Vol. 12, 2008, pp.1822–1842.
4. D. Bizzarri et. al., Propulsion vehicle integration for reusable launcher using in-flight oxygen collection, *Original Research Article, Aerosp. Sci. Technol.*, Vol. 12, No. 6, 2008, pp. 429–435.
5. H. Kubota, et al. (Toyota Industries Corporation), Exhaust Device and Exhaust Method in Internal Combustion Engine, Japanese Unexamined Patent Application Publication No.2010–196507.
6. K. Dincer et. al., Experimental investigation and exergy analysis of the performance of a counter flow Ranque-Hilsch vortex tube with regard to nozzle cross-section areas, *Int. J. Refrigeration*, Vol. 33, 2010, pp. 954–962.
7. H. Takahama, Energy Separation of Gas by Vortex Tube, *Tran. J. Soc. Mech. Eng.*, Vol. 68, No. 560, 1965, pp. 1255–1263 (in Japanese).
8. M.H. Saidi and M.S. Valipour, Experimental modeling of vortex tube refrigerator, *Appl. Therm. Eng.*, Vol. 23, pp. 1971–1980, 2003.
9. Upendra Behera et al., CFD analysis and experimental investigations towards optimizing the parameters of Ranque–Hilsch vortex tube, *Int. J. Heat Mass Transfer.*, Vol. 48, 2005, pp. 1961–1973.
10. S.U. Nimbalkar and M.R. Muller, An experimental investigation of the optimum geometry for the cold end orifice of a vortex tube, *Appl. Therm. Eng.*, Vol. 29, 2009, pp. 509–514.
11. Y.T. Wu et. al., Modification and Experimental Research on Vortex Tube, *Int. J. Refrigeration*, Vol. 30, 2007, pp.1042–1049.
12. O. Aydin and B. Markal, A New Vortex Generator Geometry for a Counter-Flow Ranque-Hilsch Vortex Tube, *Appl. Therm. Eng.*, Vol.30, 2010, pp.2505–2510.
13. B. Markal et. al., An Experimental Study on the Effect of the Valve Angle of Counter-Flow Ranque-Hilsch Vortex Tubes on Thermal Energy Separation, *Exp. Therm. Fluid Sci.*, Vol.34, 2010, pp.966–971.
14. Kun Chang et al., Experimental investigation of vortex tube refrigerator with a divergent hot tube, *Int. J. Refrigeration*, Vol. 34, 2011, pp. 322–327.
15. M. Avci, The Effects of Nozzle Aspect Ratio and Nozzle Number on the Performance of the Ranque-Hilsch Vortex Tube, *Appl. Therm. Eng.*, Vol. 50, 2013, pp.302–308.
16. Mohd Hazwan bin Yusof, Hiroshi Katanoda, and Hiromitsu Morita, Temperature and Pressure Measurements at Cold Exit of Counter-flow Vortex Tube with Flow Visualization of Reversed Flow, *Journal of Thermal Science* Vol.24(1), 2015, pp.67-72.